PROOF COPY 011207ESL

Electrochemical and Solid-State Letters, **5** (7) 1-0 (2002)
0013-4651/2002/5(7)/1/3/$7.00 © The Electrochemical Society, Inc.

Degradation of $LiNi_{0.8}Co_{0.2}O_2$ Cathode Surfaces in High-Power Lithium-Ion Batteries

Robert Kostecki* and Frank McLarnon*,z

Environmental Energy Technologies Division, Lawrence Berkeley National Laboratory, University of California, Berkeley, California 94720, USA

High-power Li-ion cells stored or cycled at elevated temperatures showed a significant impedance rise and power loss associated primarily with the $LiNi_{0.8}Co_{0.2}O_2$ cathode (positive electrode). The processes which led to this impedance rise were assessed by investigating the cathode surface electronic conductance, surface structure, and composition at the microscopic level with local probe techniques. Current-sensing atomic force microscopy imaging revealed that the cathode surface electronic conductance diminished significantly in the tested cells, and that the rate of change of the electronic conductance increased with cell test temperature. Raman microscopy measurements provided evidence that surface phase segregation of nickel oxides is at least partially responsible for the observed cathode impedance rise.
© 2002 The Electrochemical Society. [DOI: 10.1149/1.1482199] All rights reserved.

Manuscript submitted January 29, 2002; revised manuscript received April 1, 2002.

The U.S. Department of Energy's Advanced Technology Development (ATD) program supports the development of high-power Li-ion batteries for hybrid electric vehicle applications.[1] Included in the ATD program are diagnostic evaluations of Li-ion cells that were aged and/or cycled under various conditions.[2] A primary goal of these diagnostic tests is to determine the mechanisms responsible for the cell power loss that accompanies life tests at elevated temperatures. Impedance measurements of the cell components indicated that the $LiNi_{0.8}Co_{0.2}O_2$ cathode is primarily responsible for the observed cell power loss at elevated temperatures. Among the possible causes of cathode impedance rise is formation of an electronic and/or ionic barrier at the cathode surface. However, studies of the mechanism of the $LiNi_{1-y}Co_yO_2$ degradation in high-power Li-ion cells have not been reported in the literature.

Partial substitution of Co for Ni in $LiNi_{1-y}Co_yO_2$ cathodes suppresses the Jahn-Teller distortion associated with the low-spin Ni^{3+}:3d7 ion, and this substitution leads to good capacity retention and improved thermal stability when compared to the layered $LiNiO_2$ cathode.[3-5] However, $LiNi_{1-y}Co_yO_2$ cathodes still experience an inherent structural instability during long-term cycling at moderate temperatures.[6] Although $LiNiO_2$ is isostructural with $LiCoO_2$, and the Co and Ni atoms in $LiNi_{1-y}Co_yO_2$ lattice occupy equivalent sites in the R3m lattice, the electronic and coordination structures around them vary. Nakai and Nakagome[7] reported that in $Li_{1-x}Ni_{0.5}Co_{0.5}O_2$ the oxidation of Ni ions occurs immediately upon charging and halts at about $x = 0.5$, whereas the oxidation of Co ions continues to $x = 0.8$.

In this study, we investigated possible failure modes of the $LiNi_{0.8}Co_{0.2}O_2$ cathode upon storage or cycling in high-power Li-ion cells. Because X-ray diffraction spectroscopy[1] failed to detect noticeable changes in the bulk structure of the tested cathodes, we focused our attention on cathode surface processes. We demonstrated that the innovative use of noninvasive local probe techniques, such as current-sensing atomic force microscopy (AFM) and Raman microscopy, can provide unique information on surface phenomena at practical battery electrodes. These phenomena can have a dominant effect on $LiNi_{0.8}Co_{0.2}O_2$ cathode impedance behavior.

Experimental

Nine 18650 Li-ion cells were fabricated by PolyStor, Inc. for the ATD Program according to a design provided by Argonne National Laboratory (ANL) and tested at the Idaho National Engineering and Environmental Laboratory, ANL, and Sandia National Laboratories. A summary of the cell chemistry and test conditions for these cells was reported in Ref. 1 and 2. A so-called fresh cell was subjected only to formation cycles. Four cells were subjected to life-cycle testing with 3% and 9% swings in their state of charge (ΔSOC) at 60% and 80% SOC, respectively. Calendar-life tests were performed on four other cells by storing them at temperatures between 20 and 70°C.

We used current-sensing atomic force microscopy (CSAFM) to image the surface of the $LiNi_{0.8}Co_{0.2}O_2$ cathodes under a controlled N_2 atmosphere. The microscope consisted of a Molecular Imaging (MI) scanning probe microscope coupled with a Park Scientific Instruments (PSI) AutoProbe Electronic Module. The Si atomic force microscope (AFM) tips were coated with a thin conductive layer of W_2C. All CSAFM experiments were performed in constant-force mode with controlled oxide-tip voltage difference. A single scan of the tip over the cathode surface simultaneously produced two images; a topographic image and a conductance image. The latter represents oxide-tip current variations during scanning at a given oxide-tip voltage difference.

An integrated Raman microscope system "Labram" made by ISA Groupe Horiba was used to analyze the structure and composition of the $LiNi_{0.8}Co_{0.2}O_2$ cathodes. The excitation wavelength was supplied by an internal He-Ne (632 nm) 10 mW laser. The power of the laser beam was adjusted to 0.1 mW with neutral filters of various optical densities. The size of the laser beam at the sample was ~1.6 μm.

Results

Figure 1 shows CSAFM images of a representative 5 × 5 μm area of the $LiNi_{0.8}Co_{0.2}O_2$ cathodes from (A) a fresh cell, (B) a cell cycled at 40°C, 60% SOC, and 9% ΔSOC, and (C) a cell cycled at 70°C, 60% SOC, and 3% ΔSOC. The surface morphology of the fresh cathode (left) reveals well-pronounced crystal planes and edges of individual grains of the active material. Examination of the topographic AFM images of the cycled cathodes shows a significant change in the surface morphology. Considerable amounts of nanocrystalline deposit accumulated in the intergranular spaces and across the crystal planes of the active material. In our previous study we determined that the amount of deposit and the extent of morphology modification depended on the test temperatures.[2]

The right-hand panel of Fig. 1 is the oxide-tip current response (conductance image) of the same area as shown the left-hand panel at a 1.0 V voltage difference, *i.e.*, the cathode sample was poised at a positive potential *vs.* the CSAFM tip. In the conductance image, a dark color represents high electronic conductance, whereas a white color represents areas of low or zero electronic conductance. Taking into account that the tip is in physical contact with the oxide, the magnitude of the current is determined by the local electronic properties of the electrode and the tip, the tip-sample voltage difference,

* Electrochemical Society Active Member.
z E-mail: frmclarnon@lbl.gov

PROOF COPY 011207ESL

PROOF COPY 011207ESL

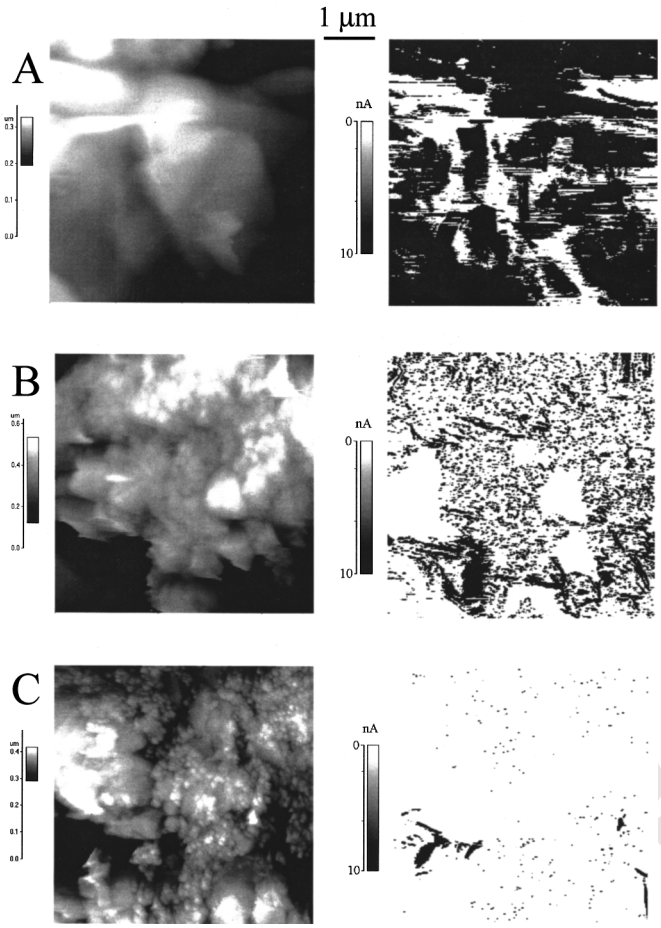

Figure 1. CSAFM images of surface conductance (right) and topography (left) of a 5 × 5 μm region of the cathode surface at 1.0 V tip-sample voltage difference. (A) virgin cell, (B) cell cycled at 40°C, 60% SOC, and 9% ΔSOC, and (C) cell cycled at 70°C, 60% SOC, and 3% ΔSOC.

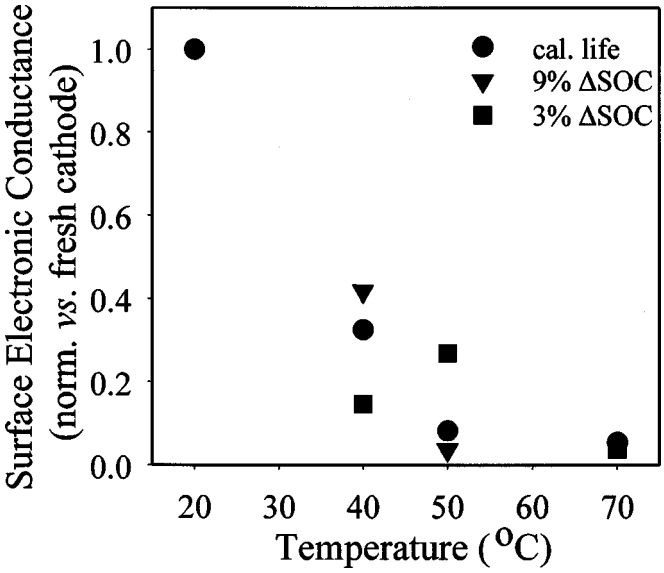

Figure 2. Average surface electronic conductance of the composite $LiNi_{0.8}Co_{0.2}O_2$ cathode normalized *vs.* the cathode from a fresh Li-ion cell. The conductivity was determined by a statistical analysis of a series of 5 × 5 μm images from different locations on the cathode surface.

and the specific geometries of the CSAFM tip and the local cathode surface. The finite dimensions of the tip (radius of curvature <30 nm) and the finite response time of the scanner electronic feedback loop may in some cases give rise to slight current variations at grain boundaries and along surface irregularities. Because the tip-to-sample current observed during imaging of the cathodes tends to switch from zero to the upper limit of the I/V converter, *i.e.*, 10 nA, depending on the location, we think that geometry factors are negligible in the conductance images presented in Fig. 1.

The surface conductance image of the cathode from the fresh cell exhibits areas of mostly excellent electronic conductance and only few insulating regions. Highly conductive graphite and acetylene black, which are present in the composite cathode, form conductive paths on the cathode surface and bulk, and are primarily responsible for the observed high tip current. The $LiNi_{0.8}Co_{0.2}O_2$ may also contribute to the tip current, but its electronic conductance is significantly lower than that of carbon. The insulating areas on the cathode surface are most likely associated with the presence of PVDF binder and/or a solid electrolyte interphase (SEI).

The conductance images of cathodes which were cycled at elevated temperatures show a dramatic increase of surface resistance. The conductance image of the cathode cycled at 40°C reveals numerous small sites with good conductance scattered across the surface. However, one can identify on the corresponding morphology image (left-hand middle panel) larger grains of cathode active material which became completely insulating. The surface electronic conductance of the cathode from the cell cycled at 70°C, deteriorated even further. Almost its entire surface became insulating except for a few locations, mainly in the deep crevices and intergranular spaces, which remained conductive.

To quantify the CSAFM results and identify a clear relationship between the cathode surface conductance changes and the cell test temperature, a statistical analysis of the CSAFM images was carried out. For every cathode a series of CSAFM images was recorded at different locations and median values of surface-average conductance were calculated. Figure 2 shows the surface-average conductance expressed *vs.* temperature. The results are normalized *vs.* the fresh cell at 20°C. It is clear from Fig. 2 that surface electronic conductance decreases monotonically with increasing cell test temperature. Interestingly, the reduction of electronic conductance was nearly identical in calendar-life cells and cycled cells. The cells tested at 70°C exhibit only 5% of their original surface electronic conductance.

To gain additional insight into the nature of the observed loss of surface electronic conductance at higher temperatures, we studied the structure and composition of the cathode surface with Raman microscopy. Figure 3 shows microraman spectra of cathodes taken from the fresh cell and the cell which was stored at 70°C. The size of the Raman probe was 1.6 μm, which is about one order of magnitude smaller that the size of an average $LiNi_{0.8}Co_{0.2}O_2$ particle. The Raman spectra of both cathodes are dominated by a group of bands between 470 and 580 cm^{-1}, characteristic for $LiNi_{0.8}Co_{0.2}O_2$ oxide. Recorded spectra of the fresh cathode were identical at all locations on the cathode surface; each spectrum consists of a broad peak centered at about 500 cm^{-1} and a sharp peak at 555 cm^{-1}. In marked contrast to the fresh cathode, the spectral characteristics the cathode stored at 70°C vary strongly as a function of location on the cathode surface, suggesting a highly nonuniform cathode surface composition and structure. The broad peak at 500 cm^{-1} split into two peaks at 475 and 550 cm^{-1}, which indicate the presence of at least partially charged $Li_{1-x}Ni_{0.8}Co_{0.2}O_2$. The cathode surface SOC varies between individual grains of active material and, at some locations, the spectra correspond to fully charged material, even though the cell was fully discharged at the end of testing and before disassembly. In addition, side peaks appear at positions close to the main peaks at 475 and 550 cm^{-1} usually associated with vibrations characteristic of the NiO_2 lattice.

PROOF COPY 011207ESL

PROOF COPY 011207ESL

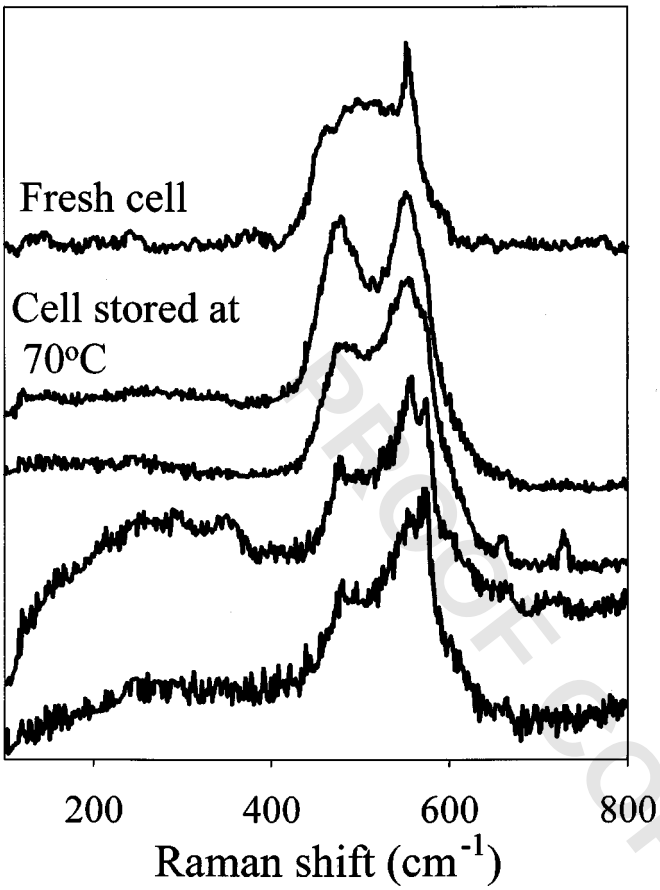

Figure 3. Microraman spectrum of the cathode from a fresh cell (upper curve), and microraman spectra from different locations on the cathode from a cell which was stored at 70°C (lower curves).

Nearly ideal substitution of Ni by either Co or Li is expressed in the Raman spectra by a slight shift of the characteristic peaks and/or their intensities. A solid solution of Li-substituted transition metal oxides can be thermodynamically unstable, particularly if one transition metal ion is preferentially oxidized. In such a case, a two-phase mixture can develop or, in the extreme case, new crystal structures can form. The lattice parameters of the $Li_{1-x}Ni_{1-y}Co_yO_2$ system increase with increasing y and decrease with increasing Li content. The development of sharp Raman peaks at positions slightly shifted from their original locations is characteristic for separate nickel oxide phases with different Co and Li contents.

A plausible explanation for the observed phenomena is Co and Ni oxide phase segregation, which was discussed in Ref. 2. It is clear that such surface processes can affect the surface electronic conductance. The Ni and Co oxide phase separation may create an additional electronic barrier at the cathode surface and thereby lead to increased electronic impedance. However, the presence of charged material at the cathode surface may also indicate that some particles of $LiNi_{0.8}Co_{0.2}O_2$ became electrically disconnected from the remaining part of the cathode due to mechanical stress, carbon additive loss, or formation of a very thin SEI layer in the cathode during testing at elevated temperatures. Ostrowskii *et al.*[8] suggested the formation of a relatively thick layer of Li_2Co_3 and P-, O-, and F-containing compounds upon storage of $LiNi_{1-y}Co_yO_2$ in $LiPF_6$-containing electrolyte at 80-90°C. Our Raman measurements as well as Midinfrared spectral (wave number range 600-4000 cm^{-1}) data revealed no observable SEI layer on the cathode surface.[2] Although we do not expect such surface processes to decrease the bulk electrode capacity to a significant extent at low cell charge and discharge rates, they may account for the substantial loss of the power observed in these cells when charged and discharged at high rates.

Acknowledgment

This research was funded by the Assistant Secretary for Energy Efficiency and Renewable Energy, Office of Advanced Automotive Technologies, U.S. Department of Energy, under contract No. DE-AC03-76SF00098. The authors gratefully acknowledge the tested cells, help, and advice provided by the ATD Program participants.

Lawrence Berkeley National Laboratory assisted in meeting the publication costs of this article.

References

1. *FY 2000 Progress Report for the Advanced Technology Development Program*, U.S. Department of Energy, Office of Advanced Automotive Technologies, Washington, D.C. (December 2000).
2. A. X. Zhang, P. N. Ross, Jr., R. Kostecki, F. Kong, S. Sloop, J. B. Kerr, K. Striebel, E. Cairns, and F. McLarnon, *J. Electrochem. Soc.*, **148**, A463 (2001).
3. W. Li and J. C. Currie, *J. Electrochem. Soc.*, **144**, 2773 (1997).
4. J. Cho, H. S. Jung, Y. C. Park, G. B. Kim, and H. S. Lim, *J. Electrochem. Soc.*, **147**, 15 (2000).
5. K-K. Lee, W-S. Yoon, and K-B. Kim, *J. Electrochem. Soc.*, **148**, A1164 (2001).
6. R. V. Chebian, F. Prado, and A. Manthiram, *J. Electrochem. Soc.*, **148**, A49 (2001).
7. I. Nakai and T. Nakagome, *Electrochem. Solid-State Lett.*, **1**, 259 (1998).
8. D. Ostrowskii, F. Ronci, B. Scrosati, and P. Jacobsson, *J. Power Sources*, **94**, 183 (2001).

PROOF COPY 011207ESL